doi:10.1093/brain/awp328 Brain 2010: 133; 482–495 | 482

BRAIN
A JOURNAL OF NEUROLOGY

The A9 dopamine neuron component in grafts of ventral mesencephalon is an important determinant for recovery of motor function in a rat model of Parkinson's disease

Shane Grealish,[1] Marie E. Jönsson,[1] Meng Li,[2] Deniz Kirik,[3] Anders Björklund[1] and Lachlan H. Thompson[1,4]

1 Division of Neurobiology, Wallenberg Neuroscience Centre, Lund University, Lund, Sweden
2 MRC Clinical Sciences Centre, Imperial College London, Hammersmith Hospital Campus, London, UK
3 Brain Repair and Imaging in Neural Systems (B.R.A.I.N.S) Unit, Department of Experimental Medical Science, Lund University, Lund, Sweden
4 Florey Neuroscience Institutes, Parkville, Victoria 3010, Australia

Correspondence to: Lachlan H. Thompson,
Florey Neuroscience Institutes,
Parkville, Victoria 3010,
Australia
E-mail: Lachlan.Thompson@florey.edu.au

Grafts of foetal ventral mesencephalon, used in cell replacement therapy for Parkinson's disease, are known to contain a mix of dopamine neuronal subtypes including the A9 neurons of the substantia nigra and the A10 neurons of the ventral tegmental area. However, the relative importance of these subtypes for functional repair of the brain affected by Parkinson's disease has not been studied thoroughly. Here, we report results from a series of grafting experiments where the anatomical and functional properties of grafts either selectively lacking in A9 neurons, or with a typical A9/A10 composition were compared. The results show that the A9 component of intrastriatal grafts is of critical importance for recovery in tests on motor performance, in a rodent model of Parkinson's disease. Analysis at the histological level indicates that this is likely to be due to the unique ability of A9 neurons to innervate and functionally activate their target structure, the dorsolateral region of the host striatum. The findings highlight dopamine neuronal subtype composition as a potentially important parameter to monitor in order to understand the variable nature of functional outcome better in transplantation studies. Furthermore, the results have interesting implications for current efforts in this field to generate well-characterized and standardized preparations of transplantable dopamine neuronal progenitors from stem cells.

Keywords: transplantation; cell therapy; substantia nigra; ventral tegmental; striatal innervation; connectivity; Pitx3

Abbreviations: E = embryonic day; GFP = green fluorescent protein; GIRK2 = G protein activated inward rectifier potassium channel-2; *Pitx3* = gene encoding pituaitary homeobox 3; TH = tyrosine hydroxylase.

Received September 3, 2009. Revised November 20, 2009. Accepted November 24, 2009

Introduction

The nigrostriatal dopamine pathway is a key regulator of motor function in the mammalian brain. The progressive loss of midbrain dopamine neurons is the leading cause of motor dysfunction in Parkinson's disease. An effective means to restore motor function in animal models of the disease, and potentially also in patients with Parkinson's disease, is to replace the missing midbrain dopamine neurons through intrastriatal transplantation of foetal ventral mesencephalic tissue (Lindvall *et al*., 1990; Björklund and Lindvall, 2000; Lindvall and Björklund, 2004). The midbrain dopamine neuroblasts, dissected from the foetal brain at the time of midbrain dopamine neurogenesis, are capable of establishing a new terminal network within the host striatum, thus restoring afferent input to striatal projection neurons and normalizing information flow through the damaged motor circuitry (Björklund *et al*., 1981; Piccini *et al*., 2000).

The midbrain dopamine neurons are a heterogeneous population and can be broadly divided into two principal subtypes, including those of the substantia nigra pars compacta and ventral tegmental area, or according to the nomenclature of Dahlstrom and Fuxe (1964), cell groups A9 and A10, respectively. Various criteria can be used to distinguish between these midbrain dopamine neuron subtypes including morphology, protein expression, target specificity and susceptibility to death in Parkinson's disease and animal models thereof. The A9 neurons are large and angular in shape, express the potassium channel subunit G protein activated inward rectifier potassium channel (GIRK)-2, project predominately to the dorsolateral striatum (corresponding to putamen and part of caudate nucleus in man), and degenerate preferentially in Parkinson's disease; while the A10 neurons are comparatively small and round in shape, many express calbindin, and they innervate ventral striatal and limbic areas, including nucleus accumbens and frontal cortex, and are relatively spared in Parkinson's disease (McRitchie *et al*., 1996; Lewis and Sesack, 1997; Damier *et al*., 1999; Mendez *et al*., 2005; Thompson *et al*., 2005). Although grafts of foetal ventral mesencephalon contain a mix of both these midbrain dopamine neuronal subtypes, the role of each of these in functional repair of the Parkinsonian brain has not been well addressed. In order to assess specifically the impact of A9 neurons, we have compared the structural and functional integration provided by intrastriatal grafts selectively lacking the A9 subtype with those of a typical mixed A9/A10 midbrain dopamine composition. This was achieved through the use of ventral mesencephalon donor tissue taken from the recently described *pituitary homeobox 3* (*Pitx3*)-green fluorescence protein (GFP) mouse, in which GFP has been knocked into the *Pitx3* gene locus (Zhao *et al*., 2004). While the midbrain dopamine neurons develop normally in mice heterozygous for GFP ($Pitx3^{WT/GFP}$), mice in which GFP has been knocked into both alleles ($Pitx3^{GFP/GFP}$) are *Pitx3* knockouts and display a phenotype in which there is selective loss of A9 neurons but sparing of A10 neurons in the midbrain (Maxwell *et al*., 2005). Results from analysis of animals grafted with either $Pitx3^{WT/GFP}$ or $Pitx3^{GFP/GFP}$ derived ventral mesencephalon tissue show that the A9 component of foetal ventral mesencephalon grafts is of critical importance for re-establishment of a new dopaminergic terminal network in the dorsolateral region of the host striatum, and restoration of motor function in an animal model of Parkinson's disease.

Materials and methods

Animals

Adult female Sprague Dawley rats (225–250 g) were used as graft recipients in these experiments and were housed on a 12 h light/dark cycle with *ad libitum* access to food and water. Adult *Pitx3*-GFP mice (Zhao *et al*., 2004), on a C5Bl6/129 background, were housed under the same conditions and used to generate embryos as a source of donor tissue for transplantation. All procedures were conducted in accordance with guidelines set by the Ethical Committee for the use of laboratory animals at Lund University.

Ventral mesencephalon cell suspensions

Timed pregnant mice [day of vaginal plug was designated embryonic day 0.5 (E0.5)] were generated by crossing male *Pitx3*-GFP mice homozygous for GFP ($Pitx3^{GFP/GFP}$) with heterozygous ($Pitx3^{WT/GFP}$) females to yield an approximately equal mix of $Pitx3^{GFP/GFP}$ and $Pitx3^{WT/GFP}$ embryos. At E12.5, embryos were removed from the pregnant females after lethal exposure to CO_2, and $Pitx3^{GFP/GFP}$ and $Pitx3^{WT/GFP}$ embryos were identified and separated under a fluorescent dissection microscope on the basis of the prominent deficit in lens development in the $Pitx3^{GFP/GFP}$ mice (Fig. 1A–B). The ventral mesencephalon was dissected from each embryo in L-15 medium (Invitrogen) as previously described (Dunnett and Björklund, 1992, 2002) and $Pitx3^{GFP/GFP}$ and $Pitx3^{WT/GFP}$ ventral mesencephalon tissue pieces were pooled in separate groups (around 20 per group). Each preparation was incubated in Hank's buffered salt solution$^{-Ca2+/Mg2+}$ (Invitrogen) containing trypsin (0.1%; Sigma) and DNase (0.05%; Sigma) for 20 min at 37°C and then mechanically dissociated into a single cell suspension as described by Nikkhah *et al.* (1994). Viable cell numbers were estimated on the basis of trypan blue (Sigma) exclusion and after centrifugation (500*g*, 5 min, 4°C), the supernatant was removed and the cells were re-suspended in Hank's buffered salt solution$^{-Ca2+/Mg2+}$ (Invitrogen) at a concentration of 0.8×10^5 ($Pitx3^{WT/GFP}$) or 1.5×10^5 ($Pitx3^{GFP/GFP}$) viable cells/μl. The cell preparations were stored on ice during the transplantation procedure.

6-Hydroxydopamine lesions and transplantation

All surgical procedures were conducted under general anaesthesia using a 20:1 fentanyl and medetomidine solution injected intraperitoneally (i.p.) (Apoteksbolaget, Sweden). The nigrostriatal dopamine pathway was partially lesioned in the host rats through intrastriatal injection of 2 μl 6-hydroxydopamine (3.5 μg/μl free base dissolved in a solution of 0.2 mg/ml L-ascorbic acid in 0.9% w/v NaCl) at each of four sites as described by Kirik *et al*. (1998), using a stereotaxic apparatus (Stoelting) and a 10 μl Hamilton syringe fitted with a glass capillary. Three weeks later, the effect of the lesion on motor function was assessed according to rotational behaviour following administration of D-amphetamine (2.5 mg/kg; i.p.), and forelimb asymmetry in the

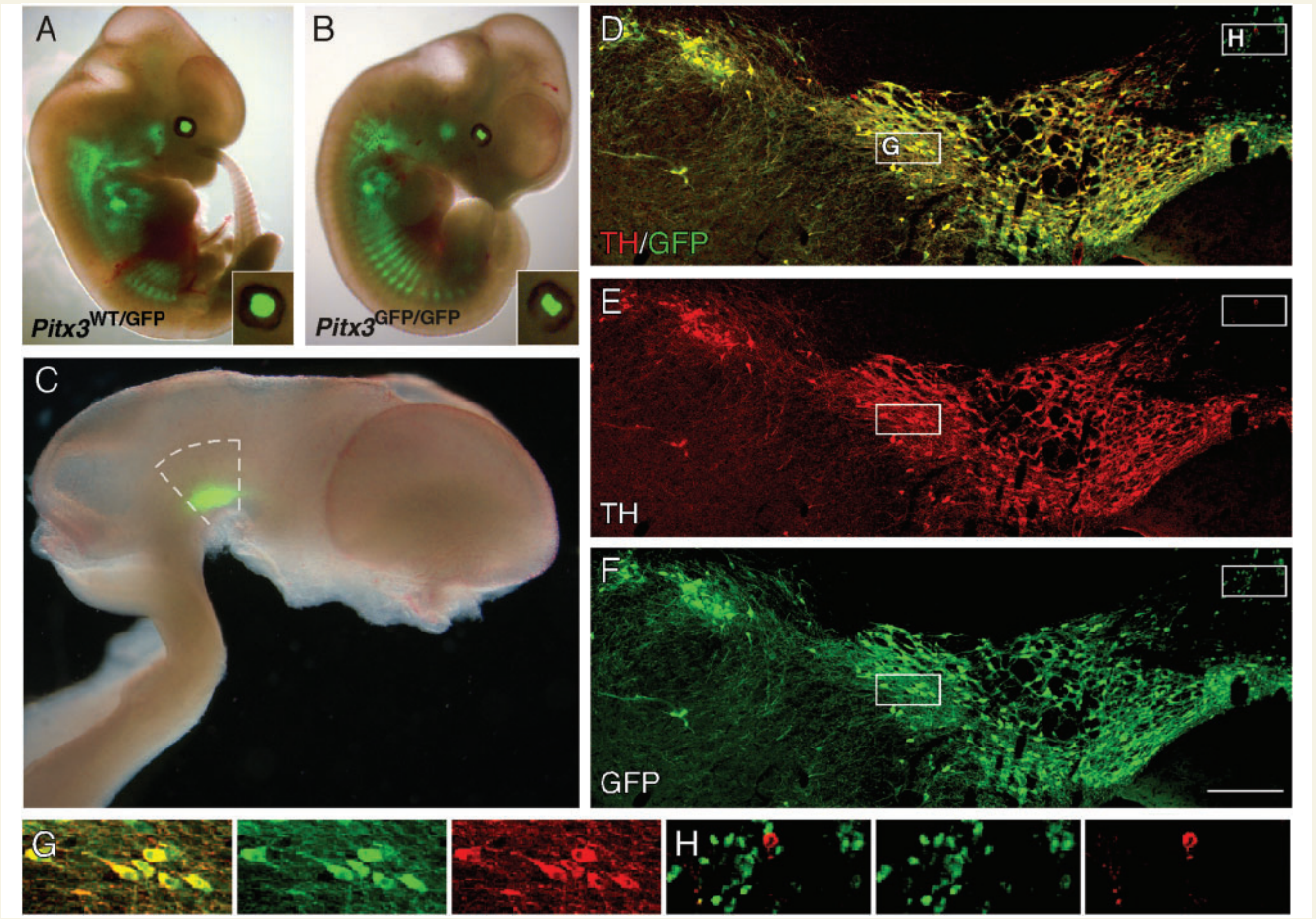

Figure 1 GFP expression in the *Pitx3*-GFP mouse. Low-magnification images show GFP expression (native emission signal) in the *Pitx3*$^{WT/GFP}$ (**A**) and *Pitx3*$^{GFP/GFP}$ (**B**) embryo (E12.5). The eyes are enlarged as insets and illustrate the malformed lens in the *Pitx3*$^{GFP/GFP}$ embryo. (**C**) In the embryonic (E12.5) brain GFP expression was seen exclusively in the ventral mesencephalon. Dashed lines indicate the area dissected for preparation of the cell suspensions used for grafting. Immunohistochemistry for GFP (green; **D**, **F**) and TH (red; **D**, **E**) shows that GFP is expressed in dopamine neurons throughout the adult midbrain. The boxed areas illustrate the morphology of GFP$^+$/TH$^+$ neurons (**G**), with large soma and neuritic processes, and also the small number of GFP$^+$/TH$^-$ cells around the midline (**H**), which were small in size and lack any obvious processes. Scale: **D–F**, 200 μm.

cylinder test. Lesioned animals were stratified across three groups ($n = 8$ per group) according to values for both behavioural measures. Limiting values for inclusion were $\geqslant 6$ turns/min (over 90 min) for rotational asymmetry and $\leqslant 25\%$ use of the forelimb contralateral to the lesion in the cylinder test. Three weeks after the behavioural pre-testing (6 weeks after lesioning) animals received intrastriatal grafts of single cell ventral mesencephalon suspension derived from either *Pitx3*$^{WT/GFP}$ ($n = 8$) or *Pitx3*$^{GFP/GFP}$ ($n = 8$) donor mice based on a micro-transplantation approach using a glass capillary attached to a 5 μl Hamilton syringe, as described by Nikkhah *et al.* (2000). A total of 1 μl of cell suspension was injected into the head of the striatum over 2 min at 0.5 mm anterior and 3.0 mm lateral to bregma, 5.0 mm below the dural surface, and the capillary was left in place a further 2 min before withdrawal. The survival time for these animals was 12 weeks, at which point the brains were processed for immunohistochemistry. Immunosuppressive treatment in the form of daily i.p. injections of cyclosporine A (15 mg/kg, Weeks 1–3; 10 mg/kg, Weeks 4–12; Novartis) was administered throughout the experiment, beginning the day prior to transplantation.

Behavioural analysis

Three weeks prior to grafting and at 8 and 12 weeks following transplantation, the two grafted groups, as well as non-grafted, lesioned ($n = 8$) and intact ($n = 6$) control groups were assessed for motor function based on amphetamine-induced rotational behaviour and cylinder testing.

Analysis of amphetamine-induced rotation was performed in automated rotational bowls (AccuScan Instruments) as described previously (Ungerstedt and Arbuthnott, 1970). D-Amphetamine sulphate was delivered (i.p.) at 2.5 mg/kg and full body rotations were recorded over a period of 90 min. The data are expressed as net full body turns per min where rotation toward the side of the lesion was given a positive value.

The cylinder test was performed as previously described (Schallert *et al.*, 2000; Kirik *et al.*, 2001) as a measure of spontaneous forelimb use. Animals were individually placed in a glass cylinder (diameter, 20 cm) and weight-bearing forepaw contacts with the glass resulting from spontaneous exploratory behaviour were recorded. A total of 20 contacts were recorded per animal and the data are presented as

the percentage of left (lesion impaired) forepaw contacts, where symmetric paw use in an unbiased animal would be 50% (10/20 contacts).

Tissue processing and immunohistochemistry

Animals received a terminal dose of 60 mg/kg sodium pentobarbitone i.p. (Apoteksbolaget, Sweden) and were trans-cardially perfused with 50 ml saline (0.9% w/v), followed by 200 ml ice-cold paraformaldehyde (4% w/v in 0.1 M phosphate buffered saline). The brains were removed, post-fixed for 2 h in 4% paraformaldehyde and cryo-protected overnight in sucrose (25% w/v in 0.1 M phosphate buffered saline) before being sectioned on a freezing microtome (Leica). Coronal sections were collected in 12 series at a thickness of 35 μm.

Immunohistochemical procedures were performed as has previously been described in detail (Thompson *et al*., 2005). Free-floating sections were incubated with primary antibodies overnight at room temperature in an incubation solution of 0.1 M phosphate buffered saline with potassium containing 5% normal serum and 0.25% Triton X-100 (Amresco, USA). Secondary antibodies were diluted in phosphate buffered saline with potassium containing 2% normal serum and 0.25% Triton X-100 and applied to the original solution for 2 h at room temperature. Detection of the primary–secondary antibody complexes was achieved by peroxidase driven precipitation of di-amino-benzidine, or conjugation of a fluorophore (either directly to the secondary antibody or with a streptavidin–biotin amplification step where necessary). For detection of c-Fos, nickel sulphate (2.5 mg/ml) was used to intensify the staining. Slide mounted sections labelled with fluorescent markers were cover-slipped with polyvinyl alcohol-1,4-diazabicyclo[2.2.2]-octane (Peterson, 1999) and di-amino-benzidine labelled sections were dehydrated in alcohol and xylene and cover-slipped with DePeX mounting media (BDH Chemicals, UK). Primary antibodies and dilution factors were as follows: mouse anti-Calbindin$_{28KD}$ (1:1000: Sigma), rabbit anti-c-Fos (1:5000, Calbiochem), chicken anti-GFP (1:1000; Abcam), rabbit anti-GFP (1:20 000; Abcam), rabbit anti-GIRK2 (1:100; Alomone Labs, Jerusalem, Israel) rabbit anti-PITX3 (1:100; Invitrogen) and mouse anti-tyrosine hydroxylase (TH: 1:4000; Chemicon). Secondary antibodies, used at a dilution of 1:200, were as follows: (i) direct detection—cyanine 3 or cyanine 5 conjugated donkey anti-mouse, cyanine 2 conjugated donkey anti-chicken, cyanine 5 conjugated donkey anti-mouse (Jackson ImmunoResearch); and (ii) indirect with streptavidin-biotin amplification—biotin conjugated goat anti-rabbit or horse anti-mouse (Vector Laboratories) followed by peroxidase conjugated streptavidin (Vectastain ABC kit, Vector laboratories), or cyanine 2/cyanine 5 conjugated streptavidin (Jackson ImmunoResearch).

Imaging

All fluorescent images were captured using a Leica DMRE confocal microscope equipped with green helium/neon, standard helium/neon and argon lasers. The macroscopic, fluorescence image of an embryonic *Pitx3*-GFP brain illustrated in Fig. 1 was acquired using a dissection microscope (Leica) equipped with a digital camera (Progres).

Densitometry

The area of re-innervated striatum around the grafts was calculated in the dorsolateral or ventromedial quadrant from two tyrosine hydroxylase-stained sections (+0.20 and −0.30 mm from bregma), as depicted in Fig. 6, using Image J software (Version 1.32j, National Institutes of Health, USA). The entire striatum was divided into quarters, and in sections where cell bodies were visible, the core of the graft was excluded from the analysis. The measured values were corrected for non-specific background staining by subtracting values obtained from the corpus callosum. The data are expressed as optical density as a percentage of the corresponding area from the intact side, and values from both sections were combined to provide a single value for each region.

Estimation of c-Fos$^+$ cell numbers

To evaluate changes in c-Fos expression in the striatal neurons, animals were sacrificed 2 h after an i.p. injection of 2.5 mg/kg D-amphetamine. High-resolution images were captured from two sections, at +0.20 and −0.30 mm from bregma, using a Scanscope GL system with Imagescope v8.2 software. A 0.8×0.8 mm^2 area medial and lateral to the graft was selected for analysis using the Image J software. The intense staining of c-Fos$^+$ nuclei and low background allowed for software-automated calculation of the total number of c-Fos$^+$ cells based on optical density upon defining the threshold for specific signal.

Cell counting

The small size of the grafts allowed for identification and counting of all GFP$^+$ dopamine neurons in each tissue series, thus avoiding the need for stereological counting procedures The total number of GFP$^+$ cells in the intrastriatal grafts was estimated for each animal through extrapolation of the number of GFP positive cells counted in every sixth coronal section. The method of Abercrombie (1946) was used to correct for double counting caused by cells spanning more than one section. Relative numbers of Calbindin$^+$/GFP$^+$, GIRK2$^+$/GFP$^+$ or Calbindin$^+$/GIRK2$^+$/GFP$^+$ cells were estimated by confocal analysis of every sixth coronal section from each animal following triple-immunohistochemical labelling for these proteins. The data are represented as the contribution of each of these three cell types to the graft as a percentage of the total number of GFP$^+$ cells expressing either GIRK2 and/or Calbindin.

Statistics

All data are expressed as mean ± the standard error of the mean. All statistical analyses were conducted using the Statistical Package for the Social Sciences 17 (SPSS Inc.). A two-tailed Student's *t*-test was used to compare the average number of GFP$^+$ cells in the two groups of grafted animals. The average density of tyrosine hydroxylase positive (TH$^+$) fibres and the number of c-Fos$^+$ cells in each group were compared using a one-way ANOVA with a Tukey *post hoc*. Two-way ANOVA was performed on all behavioural data using the generalized linear model and the Wald χ^2 followed by individual Bonferroni-corrected one-way ANOVA for each time point with Tukey *post hoc* analysis.

Results

GFP expression in the developing and adult *Pitx3*-GFP knock-in mouse

In the developing embryo, GFP expression was observed throughout the skeletal musculature, in the ventral mesencephalon and

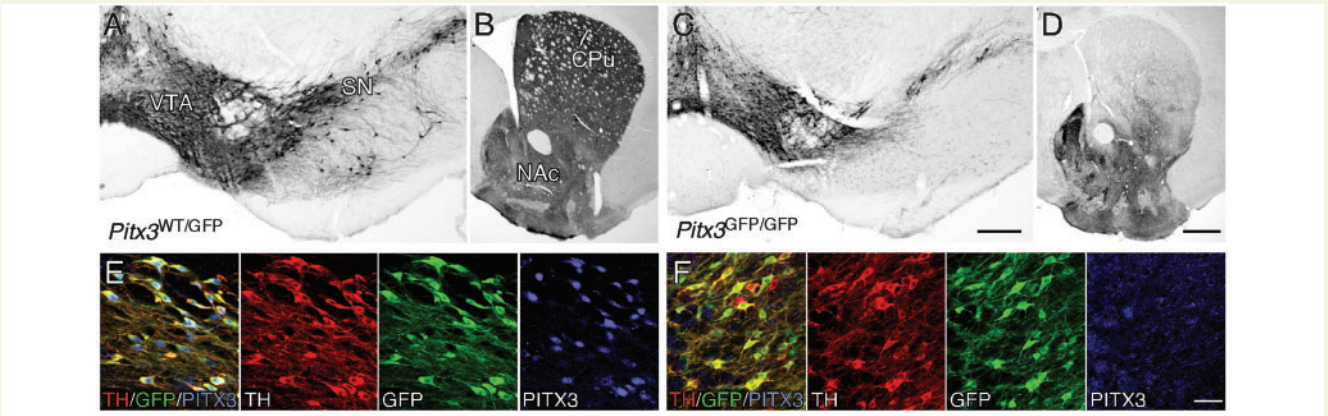

Figure 2 The *Pitx3* knockout phenotype. Immunohistochemistry for TH in the adult *Pitx3*$^{WT/GFP}$ (**A**, **B**) and *Pitx3*$^{GFP/GFP}$ (**C**, **D**) brain. In *Pitx3*$^{GFP/GFP}$ mice there was a distinct loss of TH$^+$ neurons throughout the substantia nigra (compare **A** and **C**) and a corresponding loss of TH$^+$ terminals in the dorsolateral striatum (compare **B** and **D**). Immunohistochemistry for TH (red), GFP (green) and PITX3 (blue) shows PITX3 expression in midbrain dopamine neurons in *Pitx3*$^{WT/GFP}$ mice (**E**) and lack of expression in the *Pitx3*$^{GFP/GFP}$ (*Pitx3* null) mice (**F**). CPu = caudate-putamen unit; NAc = nucleus accumbens; SN = substantia nigra; VTA = ventral tegmental area. Scale: **A** and **C**, 200 μm; **B** and **D**, 500 μm; **E–F**, 50 μm.

also in the lens (Fig. 1), as previously reported (Zhao *et al*., 2004). At E12.5, the *Pitx3*$^{GFP/GFP}$ and *Pitx3*$^{WT/GFP}$ genotypes could clearly be distinguished based on the greater intensity of GFP and also malformation of the lens in *Pitx3*$^{GFP/GFP}$ embryos (Fig. 1A and B). These features allowed for separation of the two genotypes and pooling of the ventral mesencephalons dissected from each foetus prior to preparation of the cell suspensions. In the adult brain, immunohistochemical analysis showed that GFP expression was almost exclusively confined to TH expressing dopamine neurons residing in the substantia nigra and ventral tegmental area regions of the midbrain (Fig. 1C and D). One exception was around the midline, where there were a number of GFP$^+$/TH$^-$ cells residing in the interfasicular and anterior linear raphe nuclei (Fig. 1D). When compared with the TH expressing neurons, this was a relatively minor population in number, comprising cells with a small soma and few discernable processes. Within the substantia nigra and ventral tegmental area, there was almost complete overlap between TH and GFP expression, with only some few scattered TH$^+$/GFP$^-$ neurons and no apparent TH$^-$/GFP$^+$ cells.

In order to generate mice with GFP knocked into either one (*Pitx3*$^{WT/GFP}$) or both (*Pitx3*$^{GFP/GFP}$) *Pitx3* alleles, *Pitx3*$^{GFP/GFP}$ males were bred with *Pitx3*$^{WT/GFP}$ females. This yielded mixed litters at the expected Mendelian frequency of approximately 50% for each genotype. In agreement with the original report by Maxwell and colleagues (2005), immunohistological analysis of the adult midbrain confirmed that PITX3 expression was present in *Pitx3*$^{WT/GFP}$ mice but completely abolished in *Pitx3*$^{GFP/GFP}$ littermates (Fig. 2E and F). While heterozygous *Pitx3*$^{WT/GFP}$ mice appeared indistinguishable from wild-type animals at the behavioural and histological level (not shown), the *Pitx3*$^{GFP/GFP}$ knockouts displayed a phenotype which is very similar, if not identical, to the previously described aphakia mice (Nunes *et al*., 2003; Smidt *et al*., 2004). The knockout animals were smaller in size than *Pitx3*$^{WT/GFP}$ littermates, had a small eye phenotype and histological analysis revealed a prominent loss of dopamine neurons within the substantia nigra pars compacta (Fig. 2A and C). This pattern of cell loss was reflected at the level of the striatum, where there was an almost complete loss of innervation of areas normally innervated by the A9 midbrain dopamine neurons, most notably the dorsolateral striatum, while areas innervated by A10 midbrain dopamine neurons, such as nucleus accumbens and adjacent areas of the ventromedial striatum, appeared relatively intact (Fig. 2B and D). The selective loss of A9 neurons in the *Pitx3*$^{GFP/GFP}$ knockouts was also apparent based on expression of GIRK2 and Calbindin, which are largely confined to the A9 and A10 populations, respectively (Fig. 3). While there was an almost complete loss of the GFP$^+$/GIRK2$^+$ midbrain dopamine population throughout the substantia nigra pars compacta in the *Pitx3*$^{GFP/GFP}$ mice (Fig. 3C and D), the GFP$^+$/Calbindin$^+$ midbrain dopamine neurons in the ventral tegmental area were largely spared (Fig. 3E and F). The GIRK2$^+$ neurons present in the dorsolateral part of the ventral tegmental area were also spared (Fig. 3D).

Functional impact of *Pitx3*$^{WT/GFP}$ and *Pitx3*$^{GFP/GFP}$ ventral mesencephalon grafts

We made use of ventral mesencephalon dissected from either the *Pitx3*$^{WT/GFP}$ or *Pitx3*$^{GFP/GFP}$ genetic backgrounds to prepare two different cell preparations for transplantation. Given that the midbrain in *Pitx3*$^{GFP/GFP}$ mice contains approximately half the number of midbrain dopamine neurons seen in *Pitx3*$^{WT/GFP}$ mice (Maxwell *et al*., 2005), cell suspensions were prepared such that *Pitx3*$^{GFP/GFP}$ preparations contained twice the cell concentration (1.5×10^5 cells/μl) relative to *Pitx3*$^{WT/GFP}$ preparations (0.8×10^5 cells/μl), in order to achieve grafts with a similar total number of midbrain dopamine neurons. One microlitre of cell suspension was injected into the head of striatum in intrastriatal

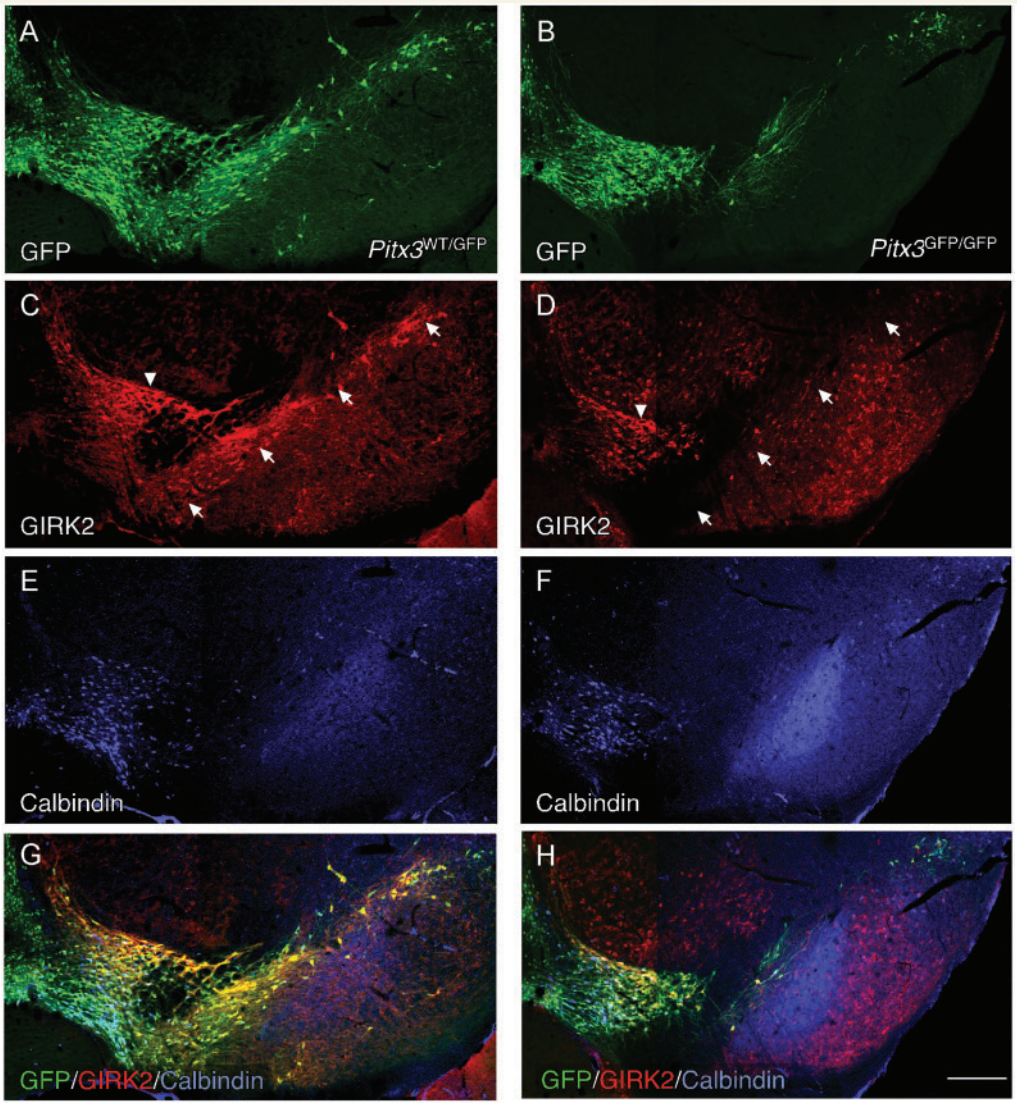

Figure 3 Subtype-specific pattern of dopamine neuronal cell loss in *Pitx3* knockouts. Immunohistochemistry for GFP (green; **A**, **B**, **G**, **H**), GIRK2 (red; **C**, **D**, **G**, **H**) and Calbindin (blue; **E**, **F**, **G**, **H**) in the adult $Pitx3^{WT/GFP}$ (**A**, **C**, **E**, **G**) and $Pitx3^{GFP/GFP}$ (**B**, **D**, **F**, **H**) brain. In the $Pitx3^{GFP/GFP}$ midbrain there was a substantial loss of the $GIRK2^{+}/GFP^{+}$ midbrain dopamine neurons throughout the substantia nigra pars compacta (arrows in **C** and **D** indicate the substantia nigra pars compacta). A population of $GIRK2^{+}$ midbrain dopamine neurons residing in the dorsolateral part of the ventral tegmental area (arrowhead in **C**, **D**) appeared to be less affected in the *Pitx3* knockout animals. The $Calbindin^{+}/GFP^{+}$ midbrain dopamine population was also left relatively intact in the $Pitx3^{GFP/GFP}$ midbrain (**E**, **F**). Scale: 200 μm.

6-hydroxydopamine lesioned rats that exhibited unilateral motor deficits, as determined by amphetamine-induced rotational behaviour and impaired forelimb use in the cylinder test. By 8 weeks post-grafting the $Pitx3^{WT/GFP}$ grafted animals showed significant reduction in rotational behaviour, while the $Pitx3^{GFP/GFP}$ grafted group and the lesion-only controls remained impaired. This effect was maintained at 12 weeks post-transplantation (Fig. 4A; group × time, $\chi^2_{(6,75)} = 27.89$, $P < 0.0001$; post-transplantation difference confirmed using a Bonferroni-adjusted one-way ANOVA with a Tukey *post hoc* test, $P < 0.05$). The $Pitx3^{WT/GFP}$ group also showed a significant improvement in performance in the cylinder test at 12 weeks compared to both lesion controls and the $Pitx3^{GFP/GFP}$ group, which did not show any sign of improvement at either time-point (Fig. 4B; group × time, $\chi^2_{(6,75)} = 38.82$, $P < 0.0001$; the difference at week 12 was confirmed using a Bonferroni-adjusted one-way ANOVA with a Tukey *post hoc* test, $P < 0.05$).

Connectivity of $Pitx3^{WT/GFP}$ and $Pitx3^{GFP/GFP}$ ventral mesencephalon grafts

Twelve weeks after transplantation, immunohistochemistry for GFP showed 8/8 and 7/8 surviving grafts in animals transplanted with $Pitx3^{WT/GFP}$ or $Pitx3^{GFP/GFP}$ cells, respectively. The vast majority of GFP expressing cells in the grafts were also TH-positive (Fig. 5A–C). As in the intact *Pitx3*-GFP midbrain, we

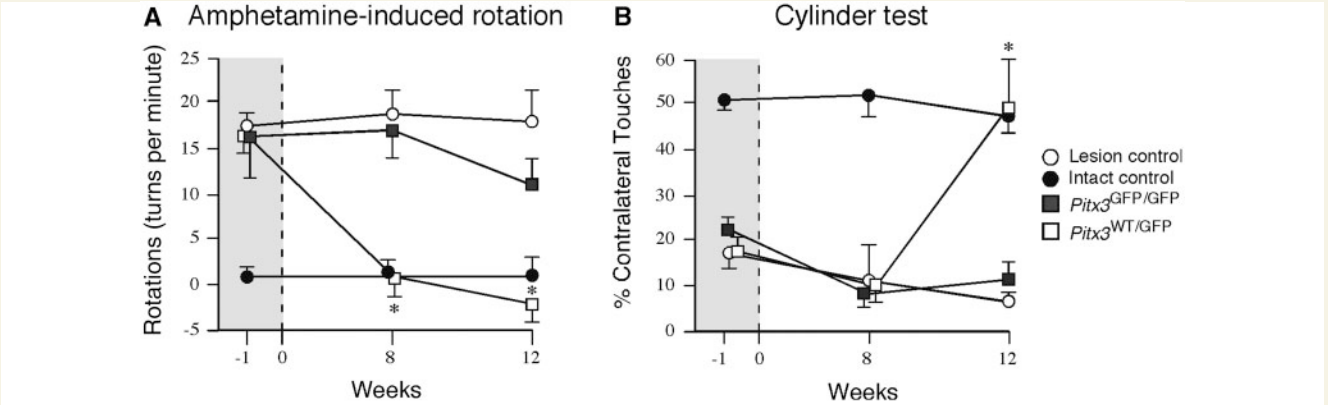

Figure 4 Functional impact of the intrastriatal grafts. Rotational behaviour in response to D-amphetamine (5 mg/kg, i.p.) prior to grafting and at 8 and 12 weeks after transplantation is shown as net rotations/minute (over 90 min) for the two grafted groups (*Pitx3*$^{WT/GFP}$, open boxes, $n=8$; *Pitx3*$^{GFP/GFP}$, grey boxes, $n=7$), as well as ungrafted intact (filled circles, $n=6$) and 6-hydroxydopamine lesioned (open circles, $n=8$) control groups (**A**). In the three lesioned groups, there was a prominent rotational bias (>15 turns/minute) in the direction ipsilateral to the 6-hydroxydopamine lesion at one week prior to transplantation. At the post-transplantation time-points only in the *Pitx3*$^{WT/GFP}$ group was the average rotational score normalized to levels significantly below the lesion control group ($^*P<0.05$). Forelimb preference in the cylinder test was assessed prior to grafting and at the same 8 and 12 week post-transplantation time-points (**B**; group numbers and symbols are the same as quoted for **A**). The intact group did not display any obvious bias for spontaneous forelimb use throughout the test procedure (on average around 50% use of the forelimb contralateral to the lesion). The three 6-hydroxydopamine lesioned groups all displayed prominent impairment in use of the contralateral forelimb (<25% use) prior to grafting. Only in the *Pitx3*$^{WT/GFP}$ group was there a significant improvement in contralateral forelimb use over the ungrafted lesion control group, and only at the 12 week time-point ($^*P<0.05$). See main text for details of statistical analyses.

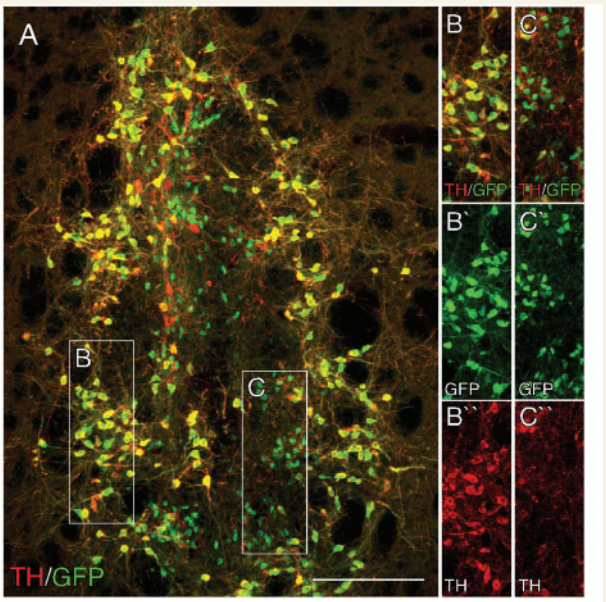

Figure 5 Expression of the GFP reporter in intrastriatal ventral mesencephalon grafts. Immunohistochemistry for GFP (green; **A–C**) and TH (red; **A–C**) in a coronal section through the striatum from a representative animal 12 weeks after transplantation of ventral mesencephalon cells from the *Pitx3*$^{WT/GFP}$ donor group. The boxed areas are shown in greater detail on the left as individual and merged colour channels and illustrate the overlap between TH and GFP that is the case for the vast majority of GFP$^+$ cells (**B**) and also the population of small TH$^-$/GFP$^+$ cells that tended to cluster in more central parts of the grafts (**C**). Scale: 200 μm.

also observed a minor population of small (<10 μm) GFP$^+$ cells that were not immunoreactive for TH (Fig. 5C). These cells had few, if any, dendritic processes and were predominately located in the central part of the graft. Counting of GFP$^+$ cells revealed that the total number of surviving midbrain dopamine neurons was not different between *Pitx3*$^{WT/GFP}$ (2517 ± 215; 3.1 ± 0.3% of cells injected) and *Pitx3*$^{GFP/GFP}$ (2079 ± 405; 1.4 ± 0.3%) grafts ($P=0.95$).

The *Pitx3* driven GFP expression could be detected not only at the level of the cell bodies but also throughout the dendritic and axonal processes of the grafted dopamine neurons. This allowed us to assess and compare the degree of graft-derived dopaminergic fibre outgrowth from *Pitx3*$^{WT/GFP}$ and *Pitx3*$^{GFP/GFP}$ grafts using GFP. Immunohistochemistry for GFP revealed a clear difference in the ability of the different graft types to innervate the host striatum. This was particularly evident in the dorsolateral region, where the *Pitx3*$^{WT/GFP}$ grafts provided extensive innervation, as a homogenous terminal network, while innervation from *Pitx3*$^{GFP/GFP}$ grafts was sparser and had a patchy appearance (Fig. 6D–E). To evaluate the ability of the different graft types to innervate the host striatum relative to that normally provided by the intact system, the density of the TH$^+$ terminal network was assessed in grafted animals from both groups and compared to TH$^+$ fibre density in the intact and lesioned striatum. Figure 6 shows TH immunohistochemistry in coronal sections from representative animals from the 6-hydroxydopamine lesion control group (A) and the *Pitx3*$^{WT/GFP}$ (B) and *Pitx3*$^{GFP/GFP}$ (C) grafted groups. The pattern of TH staining in the lesion control animal (Fig. 6A) illustrates the partial denervation induced by the intrastriatal 6-hydroxydopamine lesion. At the level of the midbrain, there was a near complete

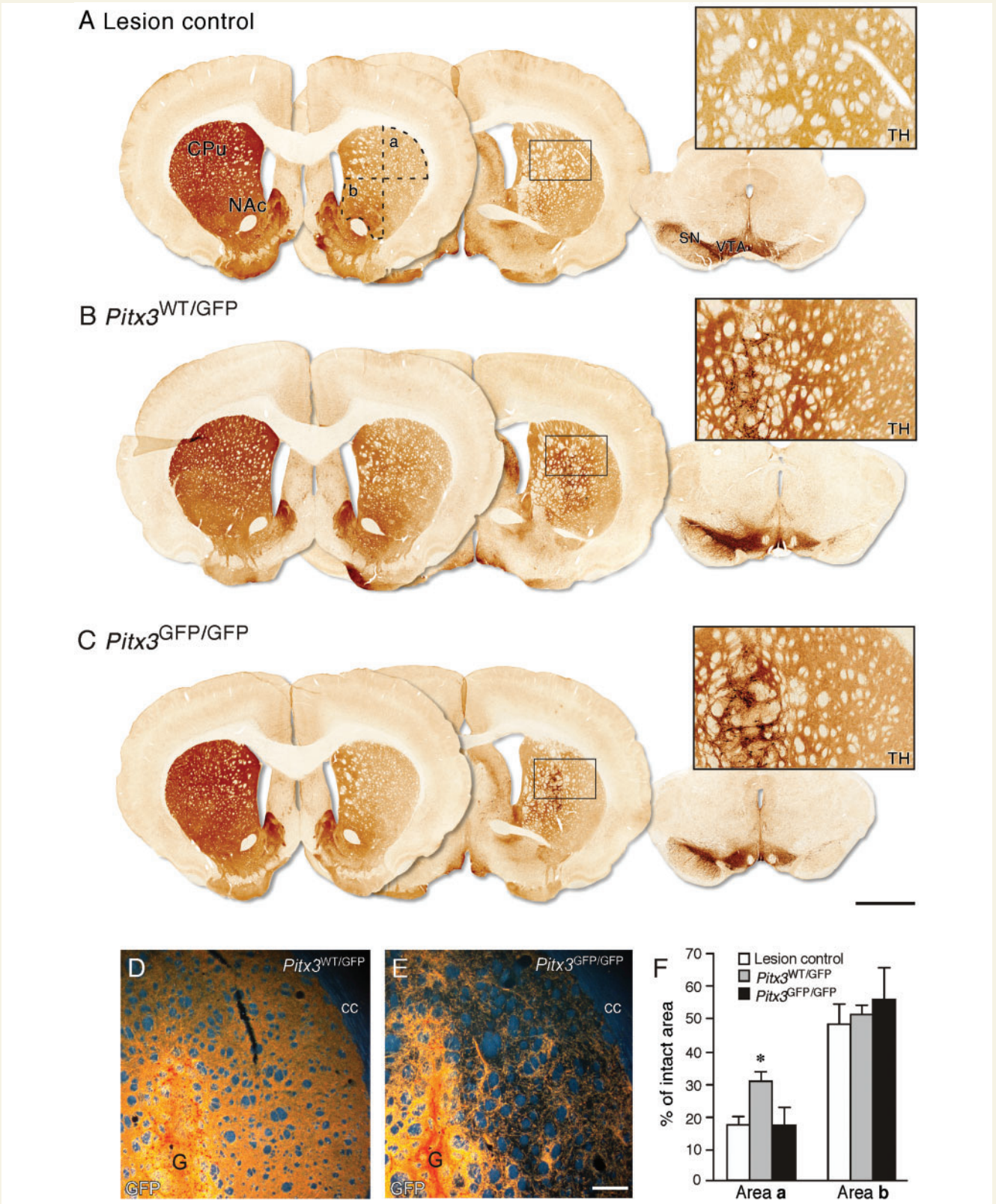

Figure 6 Connectivity of *Pitx3*$^{WT/GFP}$ and *Pitx3*$^{GFP/GFP}$ grafts. Immunohistochemistry for TH in representative coronal sections from the ungrafted lesion control (**A**), *Pitx3*$^{WT/GFP}$ graft (**B**), and *Pitx3*$^{GFP/GFP}$ graft (**C**) groups, 12 weeks after transplantation. Two sections through the forebrain (~bregma + 3.0 mm, left section and −2.0 mm, middle section) and one section through the midbrain are shown. The left-hand side of the lesion control brain shows the intact nigrostriatal projection system, while the right-hand side illustrates the substantial loss of TH^+ neurons from the substantia nigra and reduction of TH^+ terminal staining in the dorsolateral striatum resulting from the terminal 6-hydroxydopamine lesion (**A**). Dashed lines in (**A**) identify the dorsolateral (a) and ventromedial (b) quadrants of the striatum used to quantify TH^+ fibre density in the three groups. Boxed areas are enlarged and illustrate the level of TH^+ terminal staining in the

Continued

loss of TH$^+$ midbrain dopamine neurons in the substantia nigra pars compacta, while TH$^+$ neurons in the ventral tegmental area were partially spared. This was reflected in the striatum, where TH$^+$ terminal density was markedly reduced to 18 ± 3% of intact levels in the dorsolateral region (area a, Fig. 6A and F), whereas the ventromedial region was less severely dennervated (to 48.1 ± 6.5% of intact levels; area b, Fig. 6A and F). Consistent with the results obtained with GFP staining, the two different graft types displayed a marked difference in their ability to reinnervate the striatum and this was most evident in the dorsolateral region. Densitometry of TH-stained sections showed that TH$^+$ innervation in the dorsolateral striatum was significantly greater in animals grafted with *Pitx3*$^{WT/GFP}$ ventral mesencephalon (31.4 ± 2.2% of intact) when compared with animals grafted with *Pitx3*$^{GFP/GFP}$ ventral mesencephalon (18.4 ± 3.5%) or ungrafted lesioned controls (area a, Fig. 6A, B, C and F; 18.9 ± 2.4%; $F_{(2,22)} = 7.73$, $P < 0.005$; confirmed using a Tukey *post hoc* test). In the ventromedial striatum, by contrast, the TH$^+$ terminal density was not significantly increased over the average ungrafted lesion control value (48.1 ± 6.5%) in either the *Pitx3*$^{WT/GFP}$ (51.6 ± 2.7%) or the *Pitx3*$^{GFP/GFP}$ (54.3 ± 8.8%) groups [area b, Fig. 6A, B, C and F; $F_{(2,20)} = 0.24$, $P = 0.79$].

A similar region-specific difference in the striatum between the two groups of grafted animals was observed in the amphetamine-induced expression of the early immediate response gene, c-Fos (Fig. 7A–C). In the two grafted groups and also in the ungrafted, lesion control animals, the number of c-Fos$^+$ nuclei were counted in a 0.8 × 0.8 mm area medial and lateral to the graft. In a lateral part of the striatum, the average number of c-Fos$^+$ cells was similar in the *Pitx3*$^{GFP/GFP}$ (199.8 ± 19.9) and the lesion-only control groups (193.0 ± 23.4), but significantly greater in the *Pitx3*$^{WT/GFP}$ grafted animals (318.4 ± 38.6) [Fig. 7D; $F_{(3,24)} = 4.57$, $P < 0.05$, confirmed using a Tukey *post hoc* test]. In a medial part of the striatum, the average number of c-Fos$^+$ cells was not significantly different between all three groups [lesion control, 429.0 ± 61.1; *Pitx3*$^{WT/GFP}$, 355.3 ± 32.1; *Pitx3*$^{GFP/GFP}$, 352.5 ± 36.7; $F_{(3,24)} = 0.71$, $P = 0.558$].

Dopamine neuronal subtype composition of *Pitx3*$^{WT/GFP}$ and *Pitx3*$^{GFP/GFP}$ ventral mesencephalon grafts

Although the two groups of grafted animals contained similar total numbers of GFP$^+$ midbrain dopamine neurons, immunohistochemistry for GIRK2 and Calbindin revealed substantial differences in midbrain dopamine subtype composition between the two graft types. The *Pitx3*$^{WT/GFP}$ grafts contained a mix of GIRK2 and Calbindin-expressing GFP$^+$ cells such that the largest population, 65 ± 2%, was GIRK2$^+$, while 26 ± 2% were Calbindin$^+$ and 9 ± 0.3% expressed both proteins (Fig. 8A and C). The *Pitx3*$^{GFP/GFP}$ grafts, by contrast, were dominated by the calbindin$^+$ cell type (68 ± 3%), with only 15 ± 2% GIRK2$^+$, and a remaining 17 ± 2% expressing both markers (Fig. 8B and C). Both graft types also contained a small population of GFP$^+$ cells that expressed neither GIRK2 nor Calbindin and, based on size and location, most of these appeared to correspond to the small, midline population of GFP$^+$/TH$^-$ cells (data not shown).

Discussion

Previous studies have shown that grafts of foetal ventral mesencephalon tissue contain a mix of midbrain dopamine neuronal cell types including those of both the substantia nigra pars compacta (A9) and ventral tegmental area (A10) subtypes (Mendez *et al.*, 2005; Thompson *et al.*, 2005). We report here that the A9 midbrain dopamine sub-population is of critical importance for structural and functional dopamine neuron replacement in the Parkinsonian brain. To address the role of the A9 component in intrastriatal ventral mesencephalon grafts specifically, we made use of donor tissue from *Pitx3*-GFP reporter mice. The knock-in design of these mice makes possible complete deletion of the *Pitx3* gene by substitution at both alleles with GFP (*Pitx3*$^{GFP/GFP}$). Alternatively, the mice can be bred as heterozygotes, carrying copies of both the *Pitx3* and GFP genes (*Pitx3*$^{WT/GFP}$). The expression pattern of GFP in animals of either genotype was consistent with the known expression of PITX3 in the midbrain (Smidt *et al.*, 1997), lens (Semina *et al.*, 1997) and skeletal muscle (Coulon *et al.*, 2007). On closer examination of the fully developed midbrain, we found the GFP expression to match faithfully with TH expressing dopamine neurons throughout the ventral tegmental area and substantia nigra pars compacta domains of animals from both genotypes, and thus to be an excellent surrogate marker of midbrain dopamine neuronal identity. In agreement with the original description of the *Pitx3*$^{GFP/GFP}$ phenotype (Maxwell *et al.*, 2005), we observed a selective loss of substantia nigra neurons in these mice and relative sparing of ventral tegmental area neurons. This pattern of cell loss resulting from *Pitx3* deletion is consistent with the midbrain phenotype

Figure 6 Continued
dorsolateral striatum from each group. Part of the grafts, containing intensely TH$^+$ cell bodies, can be seen on the left side of the boxed panels from the two grafted groups (**B**, **C**). Darkfield photographs illustrate immunohistochemical detection of GFP in the dorsolateral striatum in *Pitx3*$^{WT/GFP}$ graft (**D**) and *Pitx3*$^{GFP/GFP}$ graft (**E**) groups. The graft core (G) can be seen in the lower left part of these panels. The average levels of TH$^+$ fibre density in the dorsolateral (area a) and ventromedial (area b) parts of the striatum are shown for the ungrafted lesion control (open bars, $n = 8$), *Pitx3*$^{WT/GFP}$ (grey bars, $n = 8$) and *Pitx3*$^{GFP/GFP}$ (black bars, $n = 7$) graft groups (**F**). The figures are given as a percentage of the TH$^+$ density values obtained in corresponding regions from the intact striatum. In the dorsolateral striatum (area a), the TH$^+$ fibre density was significantly greater in the *Pitx3*$^{WT/GFP}$ grafted group compared to the lesion control or *Pitx3*$^{GFP/GFP}$ graft groups (*$P < 0.005$). There was no significant difference in the level of TH$^+$ fibre density in the ventromedial striatum (area b) between the three groups. CPu = caudate-putamen unit; NAc = nucleus accumbens; cc = corpus callosum; G = graft; SN = substantia nigra; VTA = ventral tegmental area. See main text for details of statistical analyses. Scale: **A–C**, 2 mm; **D** and **E**, 200 μm.

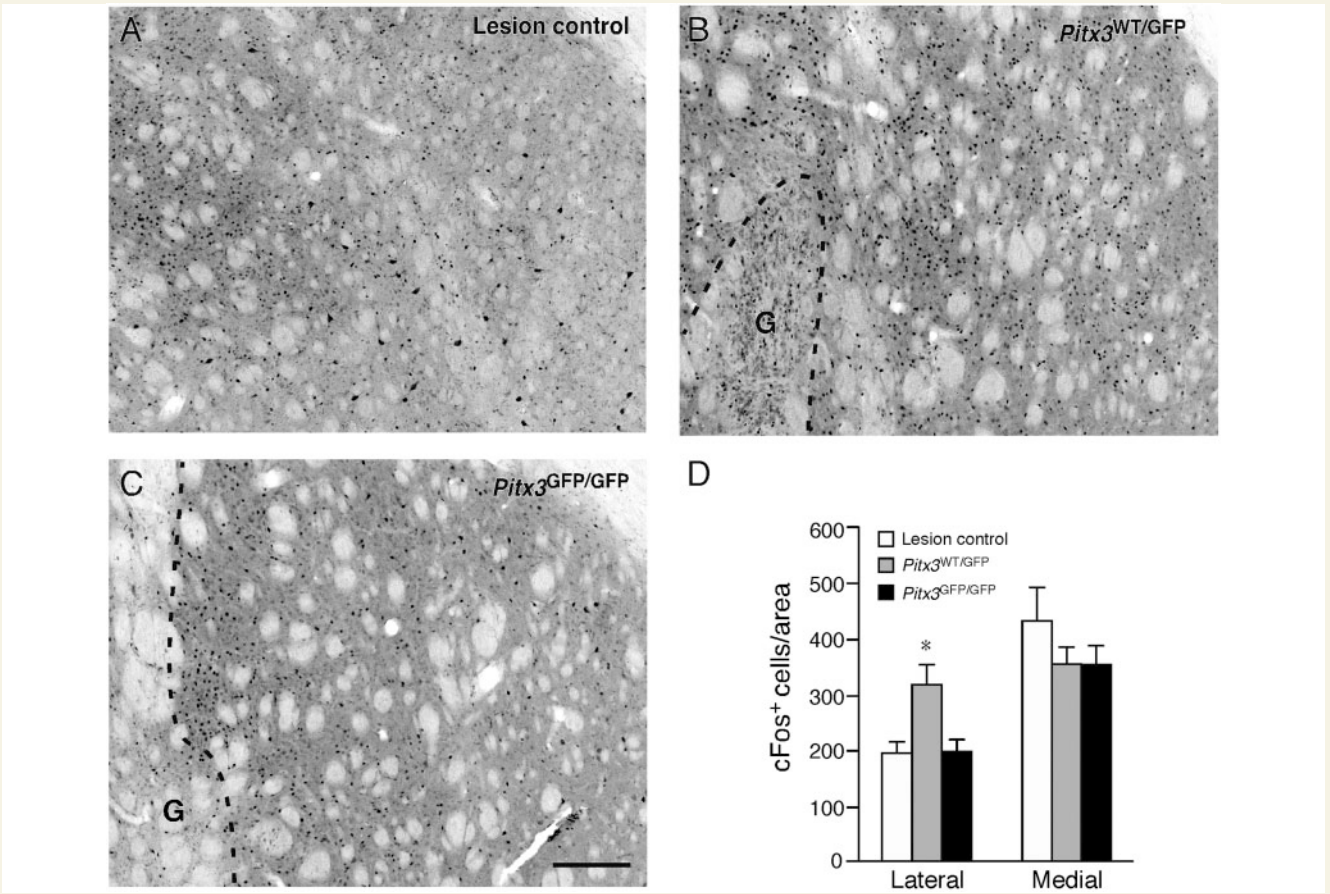

Figure 7 Activation of the post-synaptic target by *Pitx3*$^{WT/GFP}$ and *Pitx3*$^{GFP/GFP}$ grafts. Immunohistochemistry for c-Fos in the dorsolateral striatum in representative coronal sections from the ungrafted lesion control (**A**), *Pitx3*$^{WT/GFP}$ graft (**B**) and *Pitx3*$^{GFP/GFP}$ graft (**C**) groups, 12 weeks after transplantation. Dashed lines indicate the area occupied by the graft (G) in the transplanted animals. The average number of c-Fos$^+$ cells in a 0.8 × 0.8 mm area sampled from a lateral (between the graft and corpus callosum) or medial (between the graft and lateral ventricle) part of the striatum are shown for the ungrafted lesion control (open bars, $n = 8$), *Pitx3*$^{WT/GFP}$ (grey bars, $n = 8$) and *Pitx3*$^{GFP/GFP}$ (black bars, $n = 7$) graft groups (**D**). In the lateral striatum the number of c-Fos$^+$ cells was significantly greater in the *Pitx3*$^{WT/GFP}$ grafted group compared to the ungrafted control or *Pitx3*$^{GFP/GFP}$ graft groups ($^*P < 0.05$). There was no significant difference in the number of c-Fos$^+$ cells in the medial part of the striatum between the three groups. G = graft. See main text for details of statistical analyses. Scale: 200 μm.

seen in aphakia mice, which carry a loss of function mutation in the *Pitx3* gene (Nunes *et al.*, 2003; Smidt *et al.*, 2004). The selective nature of the midbrain dopamine neuronal loss was also evident based on the distribution of GIRK2$^+$ and Calbindin$^+$ cell types in the substantia nigra pars compacta and ventral tegmental area. In the intact midbrain, the expression of the GIRK2 and Calbindin proteins can broadly be used to identify the A9 and A10 midbrain dopamine populations, respectively (Mendez *et al.*, 2005; Thompson *et al.*, 2005). The majority of the A9 neurons are located within the substantia nigra pars compacta and have a GIRK2$^+$/Calbindin$^-$ phenotype, while the A10 neurons lie in the ventral tegmental area and the adjacent so-called dorsal tier of the substantia nigra, and predominately have a GIRK2$^-$/Calbindin$^+$ identity. Cells expressing both markers are found in the dorsolateral ventral tegmental area, in the transition zone between ventral tegmental area and substantia nigra. The most prominent change in the *Pitx3*$^{GFP/GFP}$ midbrain was a loss of GIRK2$^+$/Calbindin$^-$ neurons in the substantia nigra pars compacta.

Analysis of GIRK2 and Calbindin expression in the transplants of grafted animals showed that the different midbrain phenotypes of the two genetic backgrounds were closely reflected in the midbrain dopamine composition of grafts derived from either *Pitx3*$^{WT/GFP}$ or *Pitx3*$^{GFP/GFP}$ donors. The *Pitx3*$^{WT/GFP}$ grafts contained a substantial proportion of GIRK2$^+$ midbrain dopamine neurons—around 74% of all GIRK2/Calbindin expressing GFP$^+$ neurons, including 65 ± 2% GIRK2$^+$/Calbindin$^-$ and 9 ± 0.3% that expressed both proteins. The *Pitx3*$^{GFP/GFP}$ grafts, on the other hand, contained around 32% GIRK2$^+$ neurons, of which only 15 ± 2% were GIRK2$^+$/Calbindin$^-$ and 17 ± 2% expressed both GIRK2 and Calbindin. The midbrain dopamine neurons expressing both GIRK2 and Calbindin, which were found in similar numbers in both graft types, are very likely to represent the GIRK2$^+$ population found in the dorsolateral part of the ventral tegmental area, which is less affected in the *Pitx3*$^{GFP/GFP}$ midbrain. Thus, the most striking difference between the two graft types was the loss of GIRK2$^+$/Calbindin$^-$ cell types in the *Pitx3*$^{GFP/GFP}$

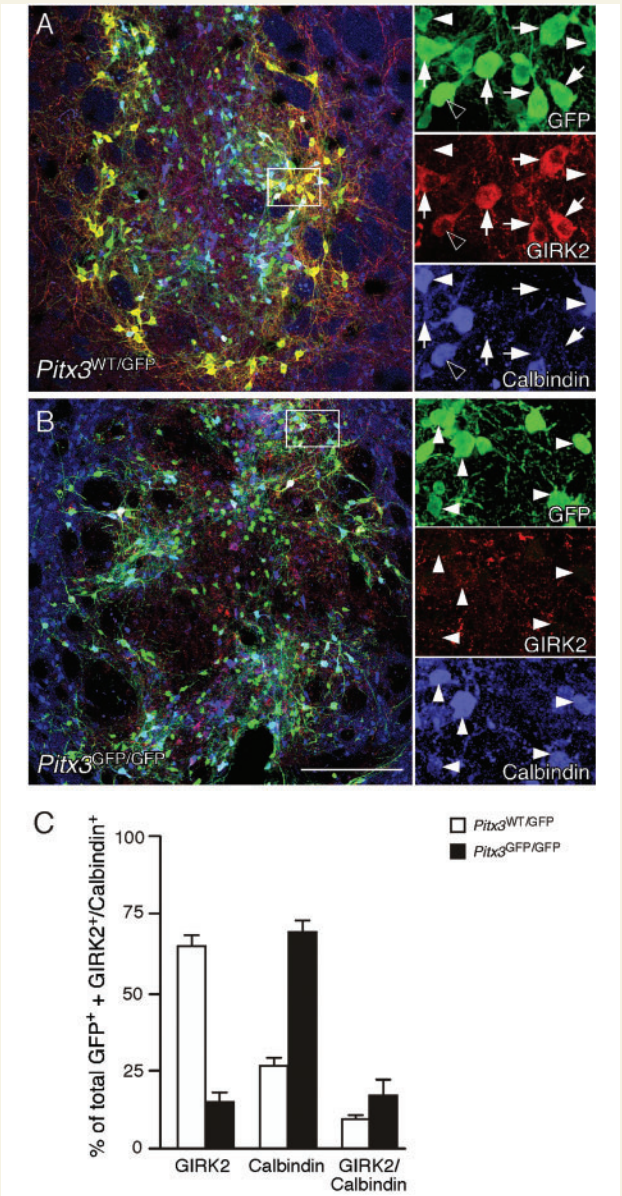

Figure 8 Subtype analysis of dopamine neurons in *Pitx3*$^{WT/GFP}$ and *Pitx3*$^{GFP/GFP}$ grafts. Immunohistochemistry for GFP (green), GIRK2 (red) and Calbindin (blue) in coronal sections through the striatum of representative animals from the *Pitx3*$^{WT/GFP}$ (**A**) and *Pitx3*$^{GFP/GFP}$ (**B**) groups, 12 weeks after transplantation. The boxed areas in the main panels are shown in greater detail as individual colour channels on the left. The *Pitx3*$^{WT/GFP}$ grafts contained a mix of GFP$^+$ midbrain dopamine subtypes including GIRK2$^+$/Calbindin$^-$ (arrows), GIRK2$^-$/Calbindin$^+$ (filled arrowheads) and GIRK2$^+$/Calbindin$^+$ (empty arrowheads) neurons. The *Pitx3*$^{GFP/GFP}$ grafts were dominated by the GIRK2$^-$/Calbindin$^+$ cell type (filled arrowheads) and contained few GIRK2$^+$ cells (not shown). Quantification of GIRK2$^+$ and Calbindin$^+$ GFP expressing neurons in all grafted animals confirmed that there was a substantial difference in the midbrain dopamine subtype composition between the two graft types, with *Pitx3*$^{WT/GFP}$ grafts ($n = 8$; open bars) containing predominately the GIRK2$^+$/Calbindin$^-$ subtype and *Pitx3*$^{GFP/GFP}$ ($n = 7$; filled bars) grafts containing mainly GIRK2$^-$/Calbindin$^+$ cells. Scale: 200 μm.

grafts, and the dominance of Calbindin$^+$ midbrain dopamine neuronal subtypes in these grafts (up to 85%, when including both Calbindin$^+$/GIRK2$^-$ and Calbindin$^+$/GIRK2$^+$ cell types), suggesting a substantially greater proportion of A10 midbrain dopamine subtypes at the expense of A9 neurons.

The *Pitx3*$^{GFP/GFP}$ grafted animals performed significantly worse in tests of motor function following grafting, relative to the *Pitx3*$^{WT/GFP}$ grafted animals. Correction of rotational asymmetry following amphetamine challenge is the most sensitive test used to assess graft function in unilateral models of Parkinson's disease. Previous studies have shown that as little as a few hundred surviving midbrain dopamine neurons are sufficient to provide a significant reduction in amphetamine-induced turning (Sauer and Brundin, 1991; Nakao *et al*., 1994; Haque *et al*., 1997). Although the number of surviving midbrain dopamine neurons seen here were well in excess of this number for both *Pitx3*$^{WT/GFP}$ (2517 ± 215) and *Pitx3*$^{GFP/GFP}$ (2079 ± 405) grafted animals, only the *Pitx3*$^{WT/GFP}$ grafted animals showed improvement in rotation scores following amphetamine challenge. This difference is readily explained by the difference in numbers of A9 neurons present in the two graft types: an average of 1638 GIRK2$^+$/Calbindin$^-$ cells (65% of 2517) in the *Pitx3*$^{WT/GFP}$ grafts versus 312 GIRK2$^+$/Calbindin$^-$ cells (15% of 2079) in the *Pitx3*$^{GFP/GFP}$ grafts. Spontaneous motor function is more resistant to graft-induced recovery, requires more extensive graft-induced reinnervation of the host striatum, and typically takes longer to manifest relative to pharmacologically induced correction of motor asymmetry (Nikkhah *et al*., 1993; Winkler *et al*., 1999). In the cylinder test, only animals in the *Pitx3*$^{WT/GFP}$ graft group showed significant improvement in contralateral forelimb use, and only at the last time point. This longer time required for correction of spontaneous motor function may reflect continued growth and maturation of the graft between 8 and 12 weeks in order, for example, to establish a threshold level of terminal innervation in the host striatum.

The ability of the two graft types to provide dopaminergic innervation to the striatum was clearly different. Analysis of GFP$^+$ or TH$^+$ fibre patterns in the grafted animals showed that the *Pitx3*$^{GFP/GFP}$ grafts had a significantly reduced capacity to establish a terminal network within the dorsolateral striatum relative to grafts derived from the *Pitx3*$^{WT/GFP}$ donors. Importantly, both groups of grafted animals contained similar numbers of midbrain dopamine neurons placed at the same intrastriatal location. Thus, the reduced striatal innervation seen in the *Pitx3*$^{GFP/GFP}$ grafts is likely to have resulted from a lower proportion of midbrain dopamine neurons of the A9 phenotype present in these grafts. Notably, the difference in innervation pattern between the two graft types, including reduced innervation of dorsolateral aspects of striatum by *Pitx3*$^{GFP/GFP}$ grafts, matched well with the different patterns of striatal innervation provided by the endogenous midbrain dopamine population in *Pitx3*$^{WT/GFP}$ and *Pitx3*$^{GFP/GFP}$ mouse brains. The normal topography of the intrinsic nigrostriatal projection to the striatum is such that the innervation of nucleus accumbens is derived predominately from ventral tegmental area midbrain dopamine neurons; the medial and ventral parts of the striatum receive projections from both ventral tegmental area and substantia nigra pars compacta neurons, and the

dorsolateral region receives innervation almost purely derived from A9 neurons in the substantia nigra pars compacta (Björklund and Lindvall, 1984). The selective loss of A9 neurons and corresponding lack of innervation of the same dorsolateral region of the striatum in both the *Pitx3*$^{GFP/GFP}$ mouse brain and in *Pitx3*$^{GFP/GFP}$ transplanted rats suggests that the normal target specificity of A9 midbrain dopamine progenitors is an intrinsic property, which is maintained after transplantation. This is in agreement with earlier studies reporting that midbrain dopamine neuronal subtypes contained in intrastriatal grafts display a remarkable capacity to innervate their appropriate developmental targets following intrastriatal grafting (Schultzberg *et al*., 1984; Haque *et al*., 1997; Thompson *et al*., 2005). Although both graft types contained large numbers of Calbindin^{+} midbrain dopamine neurons, most of which correspond to the A10 population, TH^{+} innervation of the ventromedial part of the striatum was not significantly improved above the lesion control level of around 50% in either group. This is likely to be due to the remaining intrinsic, ventral tegmental area-derived innervation of this part of the striatum in the partially lesioned animals. Previous studies have shown that the level of spared host-derived innervation of the striatum has an important impact on the ability of grafted dopamine neurons to extend axons and innervate the host (Doucet *et al*., 1989; Kirik *et al*., 2001; Thompson *et al*., 2005). In the study by Kirik *et al*. (2001), it was found that ventral mesencephalon grafts can significantly improve striatal innervation in animals where the intrinsic striatal dopamine innervation is reduced to about 20% of normal, or less, but fail to provide significant innervation in animals with moderate lesions, where the intrinsic level of innervation has not fallen below 50%. This matches well with results from the present study, where a significant level of graft-derived innervation was only achieved in the dorsolateral striatum, where the intrinsic innervation had been reduced to <20%, but not in the ventromedial striatum, which retained around half the normal level of innervation of the intact system. Thus, while target specificity of grafted midbrain dopamine neurons is largely an intrinsic property of the grafted cells, signalling from the target itself plays an important permissive role in mediating axonal growth.

In addition to investigating the significance of A9/A10 graft composition at the anatomical level, we also sought to assess how this might affect functional activation of the host striatum. To examine region-specific effects of the different graft-types within the host striatum, immunohistochemistry for c-Fos, the protein product of the early immediate response gene *c-Fos*, was performed on tissue from animals that received injection of amphetamine 2 h prior to perfusion. Expression of c-Fos has previously been shown to be up-regulated following amphetamine-induced release of dopamine from midbrain dopamine terminals in the striatum and thus providing a useful readout for functional activation of the post-synaptic target (Cenci *et al*., 1992). Increased expression of c-Fos in the dorsolateral striatum was seen only in animals that received *Pitx3*$^{WT/GFP}$ ventral mesencephalon grafts. This matches well the difference in the ability of the two graft types to reinnervate the dorsolateral striatum and is in line with the view that dopamine released from the graft-derived axon terminals is the key mediator for functional activation of the striatal target neurons. The lack of amphetamine-induced c-Fos activation in the *Pitx3*$^{GFP/GFP}$ grafted animals suggests that volume transmission, i.e. diffusion of released dopamine over distance from midbrain dopamine rich grafts is, at best, an inefficient means to normalize striatal neuron activity in the Parkinson's disease affected brain.

Taken together, these data point to an important relationship between A9/A10 midbrain dopamine subtype composition and functional impact that is mediated by the extent of graft-derived innervation of the host striatum. This is in agreement with previous findings reporting a positive correlation between the number of GIRK2^{+} neurons in intrastriatal ventral mesencephalon grafts and behavioural recovery (Kuan *et al*., 2007). It is worth noting, however, that these results do not imply that the A10 neurons are themselves unimportant for graft-mediated improvement in motor function. Recent studies have shown significantly better therapeutic outcome following ventral mesencephalon grafting in patients with preserved innervation of the ventral striatum (primarily innervated by A10 midbrain dopamine neurons) relative to those with more extensive denervation of the caudate putamen unit outside of the grafted area (Piccini *et al*., 2005), and impaired functional efficacy following grafting in rodents when the intrinsic A10-derived innervation of ventral striatal areas, including nucleus accumbens, is subsequently removed (Breysse *et al*., 2007). So while grafts with a predominately A10 composition by themselves were ineffective in our study, we cannot rule out a supportive role at the functional level for A10 neurons in mixed A9/A10 grafts. This aspect needs to be addressed in future studies.

In conclusion, the present results demonstrate the importance of midbrain dopamine neuronal subtype as a determinant of functional impact following cell-based repair of the Parkinsonian brain. A fundamental limitation imposed by the use of foetal donor tissue is the inability to standardize the cell preparations prior to grafting. In the case that procedural variations in the preparation and transplantation of foetal ventral mesencephalon tissue (donor age, dissection technique, etc) will affect the relative numbers of A9 and A10 subtypes in the resulting grafts, this may well represent an important contributing factor in the variable therapeutic outcome seen in ventral mesencephalon-grafted patients. The results also have implications for the development of novel sources of transplantable dopamine neurons. They highlight that beyond the ability to synthesize, store and release dopamine, transplanted cells should possess the capacity to re-establish a terminal network within specific regions of the caudate–putamen. Stem cells, particularly embryonic stem cells, are seen as a promising alternative to foetal tissue with the important advantage that they are more amenable to manipulation and standardization prior to grafting. Encouragingly, recent studies have shown that procedures commonly used to produce midbrain dopamine neurons from embryonic stem cells result in the production of distinct TH^{+} populations with properties of either A9 or A10 midbrain dopamine subtypes (Ferrari *et al*., 2006; Friling *et al*., 2009), and that grafting of these cells can result in extensive innervation of the host striatum, including the A9-specific dorsolateral region. None of these protocols, however, are known to direct the specification of distinct midbrain dopamine neuronal subtypes. In the protocols used currently, midbrain dopamine neuron subtypes are generated in an

uncontrolled manner as a result of patterning procedures that are more broadly geared towards generating ventralized midbrain neuronal phenotypes from neuralized embryonic stem cells. In the interest of generating highly standardized cell preparations from embryonic stem cells, our results suggest that there is considerable value in the further development of procedures that allow for the directed differentiation and/or selection of specific midbrain dopamine subtypes prior to grafting.

Acknowledgements

The authors thank Anneli Josefsson, Elsy Ling, Ulla Jarl and Bengt Mattsson for expert technical assistance.

Funding

The Swedish Research Council (04X-3874) and the Knut and Alice Wallenberg Foundation. L.T. was supported by funding from the NeuroNE Network of Excellence program of the European Union (LSHM-CT-2004-512039) and the National Parkinson Foundation (USA) Individual-Investigator grants program.

References

Abercrombie M. Estimation of nuclear population from microtome sections. Anat Rec 1946; 94: 239–47.

Björklund A, Lindvall O. Dopamine-containing systems in the CNS. In: Björklund A, Hokfelt T, editors. Handbook of chemical neuroanatomy. Vol. 2. Amsterdam: Elsevier; 1984. p. 55–123.

Björklund A, Lindvall O. Cell replacement therapies for central nervous system disorders. Nat Neurosci 2000; 3: 537–44.

Björklund A, Stenevi U, Dunnett SB, Iversen SD. Functional reactivation of the deafferented neostriatum by nigral transplants. Nature 1981; 289: 497–9.

Breysse N, Carlsson T, Winkler C, Björklund A, Kirik D. The functional impact of the intrastriatal dopamine neuron grafts in parkinsonian rats is reduced with advancing disease. J Neurosci 2007; 27: 5849–56.

Cenci MA, Kalen P, Mandel RJ, Wictorin K, Björklund A. Dopaminergic transplants normalize amphetamine- and apomorphine-induced Fos expression in the 6-hydroxydopamine-lesioned striatum. Neuroscience 1992; 46: 943–57.

Coulon V, L'Honore A, Ouimette JF, Dumontier E, van den Munckhof P, Drouin J. A muscle-specific promoter directs Pitx3 gene expression in skeletal muscle cells. J Biol Chem 2007; 282: 33192–200.

Dahlstrom A, Fuxe K. Evidence for the existence of monoamine-containing neurons in the central nervous system. I. Demonstration of monoamines in the cell bodies of brain stem neurons. Acta Physiol Scand 1964; 62 (Suppl 232): 1–55.

Damier P, Hirsch EC, Agid Y, Graybiel AM. The substantia nigra of the human brain. II. Patterns of loss of dopamine-containing neurons in Parkinson's disease. Brain 1999; 122 (Pt 8): 1437–48.

Doucet G, Brundin P, Seth S, Murata Y, Strecker RE, Triarhou LC, et al. Degeneration and graft-induced restoration of dopamine innervation in the weaver mouse neostriatum: a quantitative radioautographic study of [3H]dopamine uptake. Exp Brain Res 1989; 77: 552–68.

Dunnett SB, Björklund A. Staging and dissection of rat embryos. In: Dunnnet SB, Björklund A, editors. Neural transplantation. A practical approach. Oxford: Oxford University Press; 1992. p. 1–18.

Dunnett SB, Björklund A. Dissecting embryonic neural tissues for transplantation. In: Dunnett SB, Boulton AA, Baker GB, editors. Neuromethods: cell and tissue transplantation in the CNS. Totowa: Humana Press; 2000. p. 3–25.

Ferrari D, Sanchez-Pernaute R, Lee H, Studer L, Isacson O. Transplanted dopamine neurons derived from primate ES cells preferentially innervate DARPP-32 striatal progenitors within the graft. Eur J Neurosci 2006; 24: 1885–96.

Friling S, Andersson E, Thompson LH, Jonsson ME, Hebsgaard JB, Nanou E, et al. Efficient production of mesencephalic dopamine neurons by Lmx1a expression in embryonic stem cells. Proc Natl Acad Sci USA 2009; 106: 7613–8.

Haque NS, LeBlanc CJ, Isacson O. Differential dissection of the rat E16 ventral mesencephalon and survival and reinnervation of the 6-OHDA-lesioned striatum by a subset of aldehyde dehydrogenase-positive TH neurons. Cell Transplant 1997; 6: 239–48.

Kirik D, Rosenblad C, Björklund A. Characterization of behavioral and neurodegenerative changes following partial lesions of the nigrostriatal dopamine system induced by intrastriatal 6-hydroxydopamine in the rat. Exp Neurol 1998; 152: 259–77.

Kirik D, Winkler C, Björklund A. Growth and functional efficacy of intrastriatal nigral transplants depend on the extent of nigrostriatal degeneration. J Neurosci 2001; 21: 2889–96.

Kuan WL, Lin R, Tyers P, Barker RA. The importance of A9 dopaminergic neurons in mediating the functional benefits of fetal ventral mesencephalon transplants and levodopa-induced dyskinesias. Neurobiol Dis 2007; 25: 594–608.

Lewis DA, Sesack SR. Dopamine systems in the primate brain. In: Bloom FE, Björklund A, Hokfelt T, editors. Handbook of Chemical Neuroanatomy. Vol. 13. Amsterdam: Elsevier; 1997. p. 263–375.

Lindvall O, Björklund A. Cell therapy in Parkinson's disease. NeuroRx 2004; 1: 382–393.

Lindvall O, Brundin P, Widner H, Rehncrona S, Gustavii B, Frackowiak R, et al. Grafts of fetal dopamine neurons survive and improve motor function in Parkinson's disease. Science 1990; 247: 574–7.

Maxwell SL, Ho HY, Kuehner E, Zhao S, Li M. Pitx3 regulates tyrosine hydroxylase expression in the substantia nigra and identifies a subgroup of mesencephalic dopaminergic progenitor neurons during mouse development. Dev Biol 2005; 282: 467–79.

McRitchie DA, Hardman CD, Halliday GM. Cytoarchitectural distribution of calcium binding proteins in midbrain dopaminergic regions of rats and humans. J Comp Neurol 1996; 364: 121–50.

Mendez I, Sanchez-Pernaute R, Cooper O, Vinuela A, Ferrari D, Björklund L, et al. Cell type analysis of functional fetal dopamine cell suspension transplants in the striatum and substantia nigra of patients with Parkinson's disease. Brain 2005; 128: 1498–510.

Nakao N, Frodl EM, Duan WM, Widner H, Brundin P. Lazaroids improve the survival of grafted rat embryonic dopamine neurons. Proc Natl Acad Sci USA 1994; 91: 12408–12.

Nikkhah G, Cunningham MG, Jodicke A, Knappe U, Björklund A. Improved graft survival and striatal reinnervation by microtransplantation of fetal nigral cell suspensions in the rat Parkinson model. Brain Res 1994; 633: 133–43.

Nikkhah G, Duan WM, Knappe U, Jodicke A, Björklund A. Restoration of complex sensorimotor behavior and skilled forelimb use by a modified nigral cell suspension transplantation approach in the rat Parkinson model. Neuroscience 1993; 56: 33–43.

Nikkhah G, Winkler C, Rödter A, Samii M. Microtransplantation of nigral dopamine neurons: a ''step by step'' recipe. In: Dunnett SB, Boulton AA, Baker GB, editors. Neuromethods: Cell and Tissue Transplantation in the CNS. Totowa: The Human Press; 2000. p. 207–31.

Nunes I, Tovmasian LT, Silva RM, Burke RE, Goff SP. Pitx3 is required for development of substantia nigra dopaminergic neurons. Proc Natl Acad Sci USA 2003; 100: 4245–50.

Peterson DA. The use of fluorescent probes in cell counting procedures. In: Janson A M, Evans SM, Möller A, editors. Quantitative methods in neuroscience – a neuroanatomical approach. Vol. 36. Oxford: Oxford University Press; 1999. p. 86–115.

Piccini P, Lindvall O, Björklund A, Brundin P, Hagell P, Ceravolo R, et al. Delayed recovery of movement-related cortical function in Parkinson's disease after striatal dopaminergic grafts. Ann Neurol 2000; 48: 689–95.

Piccini P, Pavese N, Hagell P, Reimer J, Björklund A, Oertel WH, et al. Factors affecting the clinical outcome after neural transplantation in Parkinson's disease. Brain 2005; 128: 2977–86.

Sauer H, Brundin P. Effect of cool storage on survival and function of intrastriatal ventral mesencephalic grafts. Restor Neurol Neurosci 1991; 2: 123–35.

Schallert T, Fleming SM, Leasure JL, Tillerson JL, Bland ST. CNS plasticity and assessment of forelimb sensorimotor outcome in unilateral rat models of stroke, cortical ablation, parkinsonism and spinal cord injury. Neuropharmacology 2000; 39: 777–87.

Schultzberg M, Dunnett SB, Björklund A, Stenevi U, Hokfelt T, Dockray GJ, et al. Dopamine and cholecystokinin immunoreactive neurons in mesencephalic grafts reinnervating the neostriatum: evidence for selective growth regulation. Neuroscience 1984; 12: 17–32.

Semina EV, Reiter RS, Murray JC. Isolation of a new homeobox gene belonging to the Pitx/Rieg family: expression during lens development and mapping to the aphakia region on mouse chromosome 19. Hum Mol Genet 1997; 6: 2109–16.

Smidt MP, Smits SM, Bouwmeester H, Hamers FP, van der Linden AJ, Hellemons AJ, et al. Early developmental failure of substantia nigra dopamine neurons in mice lacking the homeodomain gene Pitx3. Development 2004; 131: 1145–55.

Smidt MP, van Schaick HS, Lanctot C, Tremblay JJ, Cox JJ, van der Kleij AA, et al. A homeodomain gene Ptx3 has highly restricted brain expression in mesencephalic dopaminergic neurons. Proc Natl Acad Sci USA 1997; 94: 13305–10.

Thompson L, Barraud P, Andersson E, Kirik D, Björklund A. Identification of dopaminergic neurons of nigral and ventral tegmental area subtypes in grafts of fetal ventral mesencephalon based on cell morphology, protein expression, and efferent projections. J Neurosci 2005; 25: 6467–77.

Ungerstedt U, Arbuthnott GW. Quantitative recording of rotational behavior in rats after 6-hydroxy-dopamine lesions of the nigrostriatal dopamine system. Brain Res 1970; 24: 485–93.

Winkler C, Bentlage C, Nikkhah G, Samii M, Björklund A. Intranigral transplants of GABA-rich striatal tissue induce behavioral recovery in the rat Parkinson model and promote the effects obtained by intrastriatal dopaminergic transplants. Exp Neurol 1999; 155: 165–86.

Zhao S, Maxwell S, Jimenez-Beristain A, Vives J, Kuehner E, Zhao J, et al. Generation of embryonic stem cells and transgenic mice expressing green fluorescence protein in midbrain dopaminergic neurons. Eur J Neurosci 2004; 19: 1133–40.